Linking TreeQSM with SAR and ALS to Detect Internal Canopy Allocation Shifts Across Scales

Hanna Sorokina[1], Mariana Campos[1], Taiga Korpelainen[2], Rami Echriti[1], Eetu Puttonen[1], Juha Hyyppä[1], Yunsheng Wang[1]

[1] Finnish Geospatial Research Institute, National Land Survey of Finland. Vuorimiehentie 5, 02150 Espoo – hanna.sorokina@nls.fi, mariana.campos@nls.fi, rami.echriti@nls.fi, eetu.puttonen@nls.fi, juha.hyyppa@nls.fi, yunsheng.wang@nls.fi
[2] Department of Geosciences and Geography, University of Helsinki. Fabianinkatu 33, 00014 University of Helsinki. – taiga.korpelainen@helsinki.fi

Keywords: Synthetic Aperture Radar (SAR), Airborne Laser Scanning (ALS), TreeQSM, Canopy Structure, Branch Allocation, Multi-Temporal Analysis.

Abstract

Linking remotely sensed forest backscatter with fine-scale tree crown structural dynamics provides insights into tree growth strategies under varying conditions. In this study, we investigate whether branch-scale tree growth allocation dynamics, derived from multi-temporal TreeQSM models, are reflected in SAR and ALS observations. We analyzed branch organization dynamics of silver birch (*Betula pendula*) using terrestrial laser scanning data from 2021, 2023 and 2025 at a boreal forest site in southern Finland. Branch allocation metrics, including volume-weighted mean diameter (VWMD), small branch fraction (SBF), distal volume fraction, relative branch height, and top canopy volume, were quantified to capture shifts between structural reinforcement and exploratory growth. These metrics were compared with Sentinel-1 SAR features (α, entropy, C_{11}, C_{22}) and ALS-derived canopy metrics (plant area index, vertical complexity index) alongside local structural variables. Results show a consistent trade-off between coarse and fine branching, with strong negative correlations between ΔVWMD and ΔSBF across both periods ($\rho = –0.92$). SAR-derived α exhibits strong associations with these allocation shifts during 2021–2023 ($\rho = –0.81$ with ΔVWMD; $\rho = 0.75$ with ΔSBF), indicating sensitivity to internal redistribution of branch material. ALS metrics from 2021 reflect initial canopy structure and are associated with subsequent allocation shifts. Despite the small magnitude of observed changes, consistent monotonic relationships across datasets suggest that subtle within-crown branch allocation is detectable from satellite and aerial observations, reflecting the surrounding canopy context. However, weakened correlations in 2023–2025 highlight the influence of external factors on SAR signals.

1. Introduction

Tree crowns are dynamic systems shaped by growth processes and environmental conditions, where their structural attributes such as branch size, distribution, and spatial arrangement reflect and influence both tree function and canopy-level properties. Therefore, understanding how trees adjust their branching architecture over time provides essential insights into growth strategies, resource allocation, and structural adaptation to environmental conditions (Seidel et al., 2011).

Advances in LiDAR-based monitoring, especially at close-range with terrestrial laser scanning (TLS), have enabled increasingly detailed characterization of tree structure. Previous studies have demonstrated that tree crown geometry and branching architecture can be reconstructed with high accuracy (Wilkes et al., 2021), while studies focusing on temporal changes in tree structure at branch-level are still limited. Branch dynamics such as water-induced branch movement have been observed with TLS time-series (Junttila et al., 2022). More recently, multi-temporal LiDAR data have also enabled analysis of tree architecture at the branch scale, using quantitative structure models (QSMs) that allow direct quantification of structural attributes such as branch diameter and volume (Sorokina et al., 2026).

Despite recent advancements in LiDAR time-series observations in terms of spatial and temporal resolution, investigations of branch-level crown structure dynamics remain limited, even though such dynamics are essential for understanding tree functioning processes. Changes in the allocation of branch material within the crown, such as shifts between finer and coarser structural elements, are difficult to capture and quantify, thus, are rarely assessed directly. Consequently, exploring how these changes are reflected in airborne or even satellite observations at larger spatial scales is even more complex and remains a key challenge for forest monitoring.

Remote sensing approaches have been widely used to characterize forest structure at larger spatial scales. Airborne laser scanning (ALS) provides information on canopy height, density, and vertical structure (Bruggisser et al., 2019), while synthetic aperture radar (SAR), particularly in its polarimetric form, captures information related to canopy scattering mechanisms and structural complexity (Cloude and Pottier, 1997). However, SAR-based observations are typically interpreted in terms of bulk canopy or stand-level properties (e.g., Dostálová et al., 2018; Proisy et al., 2000; Rüetschi et al., 2018), and their sensitivity to within-crown changes at the branch level remains unclear.

With the rapidly increasing availability of close-range sensing technologies, such as TLS, new opportunities have emerged to bridge fine-scale tree structural dynamics with large-scale remote sensing observations. Close-range measurements from TLS can capture detailed branch- and stem-level structural changes with high precision, while aerial and satellite platforms provide broader spatial coverage. If successfully bridged and linked, it would enable the upscaling of detailed tree-level dynamics to landscape- and regional-scale perspectives.

In this study, we investigate multi-temporal changes in branch-level structural attributes derived from TreeQSM models of silver birch (*Betula pendula*) and examine their relationships with SAR and ALS observations. Specifically, we (i) quantify changes in branch allocation metrics between time periods, (ii) analyze their associations with SAR-derived scattering parameters and ALS-derived canopy metrics, and (iii) evaluate the extent to which branch-level structural changes are reflected in remote sensing signals.

2. Data and Methods

2.1 Study Data

The study integrates terrestrial laser scanning (TLS) point cloud data, Sentinel-1 SAR data, and airborne laser scanning (ALS)-derived canopy metrics to analyze structural allocation in trees. TLS data from the LiPhe station were used to reconstruct detailed tree architecture using TreeQSM. Sentinel-1 SAR data were used to characterize canopy scattering properties, and ALS-derived metrics were used to describe canopy density and structural complexity at the site level.

The TLS data was collected from the permanent LiDAR phenology station (LiPhe) at the Hyytiälä Forest Station in Southern Finland (61°51′N, 24°17′E). The hyper temporal laser scanner is installed 30 meters above the ground in a flux tower. The scanner captures the 3D structure of the surrounding forest on an hourly basis. Technical details of the LiPhe station can be found from Campos et al. (2021) and Sorokina et al. (2026). The data is available from Wittke et al. (2024).

The analysis was conducted for the periods 2021–2023 and 2023–2025 to capture structural changes over multi-year intervals. A single representative scan per year was used for TreeQSM reconstruction, ensuring consistency in acquisition conditions and comparability of derived structural metrics across the study periods. Although LiPhe provides hourly observations, changes were analyzed over multi-year intervals because this allows more robust detection of allocation shifts.

For each study year, point cloud data were selected from early April acquisitions (2.4.2021, 7.4.2023, and 6.4.2025), corresponding to comparable seasonal conditions across years. The focus on leaf-off silver birch reflects previous findings (Sorokina et al., 2026) that leaf removal leads to loss of branches in QSMs, thereby compromising the structural realism.

To minimize the influence of wind-induced movement on branch reconstruction, scans were chosen from early evening periods (approximately 18:00–19:00), when wind conditions were low (wind speed below 3 m/s). From the LiPhe study area, we initially selected 69 representative silver birch trees, with final sample selection based on TreeQSM reconstruction quality (Section 2.2).

The individual tree delineation process (semi-automated coarse-to-fine approach) is described in detail by Sorokina et al. (2026). Subsequent fine segmentation was performed by manually removing noise from nearby trees, shrubs, and ground using CloudCompare (CloudCompare, 2021) to include only woody structures of individual trees. Additionally, statistical outlier (SOR) filter was applied to enhance the point cloud data quality by removing points far away from their neighbors.

Sentinel-1 (S1) SAR data (SLC IW mode; native resolution approximately 5 × 20 m in range and azimuth, resampled to a 10 m grid during terrain correction; ascending orbit; relative orbit 160) were acquired for early April for each study year (6.4.2021, 8.4.2023, and 9.4.2025), corresponding closely to the timing of TreeQSM data collection (2.4.2021, 7.4.2023, and 6.4.2025).

The ALS campaign was conducted in 2021. The campaign used the FGI HeliALS-TW system, which consists of a RIEGL VUX-1HA scanner (RIEGL Laser Measurement Systems GmbH, Horn, Austria) that is integrated onto a helicopter platform. Technical details of the system can be found from Korpelainen et al. (2026).

2.2 TreeQSM Generation

TreeQSM v2.4.1 modeling tool (Raumonen and Åkerblom, 2024) implemented in MATLAB (The MathWorks Inc., 2024) was used to generate QSMs for individual trees.

QSMs are cylinder-based hierarchical representations of tree architecture, in which the woody structure is reconstructed as a connected set of cylinders approximating the stems and branches. QSMs enable detailed quantification of branch-level geometry, including diameter, length, volume, and spatial arrangement within the canopy.

Only QSMs of sufficient structural quality were included in the analysis. A model was considered acceptable if the main stem was continuously reconstructed from the base to the upper crown, and the overall branching architecture appeared coherent and free of major artifacts (e.g., disconnected segments or unrealistic branching patterns). Minor imperfections, such as small gaps in fine branches and slight over- or under segmentation of branch elements, were tolerated, as some level of reconstruction uncertainty is inherent to the modeling process. This restricted the initial sample of 69 birches to a small set of birches (n = 11) for which TreeQSM reconstructions were consistently deemed acceptable for all time points (2021, 2023, and 2025), ensuring more reliable representation of branch structure. The average height of these 11 birches was 18.23 m in 2021 and 18.86 m in 2025.

https://doi.org/10.5194/isprs-archives-XLIX-B1-2026-457-2026

2.3 Branch Allocation Metrics

TreeQSM-derived metrics were selected to capture complementary aspects of branch-level structural allocation within the canopy.

Branch allocation was characterized using volume-based metrics, describing how structural investment is distributed within the tree. Volume-weighted mean diameter (VWMD, m) represents structural investment in coarse, load-bearing branches, with higher values indicating a shift toward thicker structural elements.

Distal volume fraction (DVF, unitless) quantifies allocation to higher-order branches (≥3), reflecting investment toward the outer, exploratory parts of the crown. Small branch fraction (SBF, unitless) captures the proportion of volume in fine branches (<0.05 m), indicating allocation to finer, more dynamic or short-lived structures.

Vertical allocation is described using cylinder-derived metrics. Relative branch height (RBH, unitless) represents the average vertical position of branch volume within the tree, with higher values indicating a concentration of biomass higher in the crown. Top canopy volume (TCV, unitless) quantifies the proportion of branch volume located in the upper third of tree height, reflecting allocation toward the upper canopy layer.

Together, these metrics provide a concise representation of internal canopy organization and enable quantification of allocation shifts between structural reinforcement and exploratory growth.

2.4 SAR Processing and Feature Extraction

Sentinel-1 SAR data from 2021, 2023, and 2025 were processed using the SARP (Sentinel-1 Automated Retrieval and Processing) pipeline (Mäkinen, 2024) on the Puhti supercomputer (CSC – IT Center for Science, Finland) for SAR data retrieval and processing, enabling consistent retrieval of backscatter and polarimetric features.

The polarimetric alpha angle (α) describes dominant scattering mechanisms, ranging from surface to volume and double bounce scattering (Cloude and Pottier, 1997). Entropy (H) represents the randomness of scattering within the canopy, indicating the degree of heterogeneity in the distribution of scattering elements. Backscatter coefficients (covariance matrix components C_{11} and C_{22}), corresponding to co- and cross-polarized returns, reflect contributions from more coherent structures and volume scattering, respectively. These were converted from linear scale to decibels (dB), and their difference (C_{22}–C_{11}) was calculated to capture relative scattering contributions.

For each tree, mean SAR values were extracted within a 3 m buffer around the tree location, corresponding to a 6 m diameter and 28.27 m^2 crown area, which slightly exceeds the observed TreeQSM canopy extent to ensure coverage under uncertainty. The average maximum TreeQSM-derived canopy diameter in 2025 for the 11 birches is 3.33 m, with the largest maximum diameter being 4.54 m. However, tree crowns may not be perfectly centered around the stem location. The canopy buffers therefore extend beyond the crown boundary to account for possible crown asymmetry and positional uncertainty. The canopy buffers cover multiple SAR pixels, with an average cell count of 2.57 pixels per tree.

The buffer size also mitigates spatial uncertainty in SAR geolocation by reducing sensitivity to small positional offsets between the tree location and the SAR pixel grid, which may arise from geolocation uncertainties during terrain correction. While the buffer size remains smaller than the effective SAR resolution, it provides a consistent sampling unit for linking tree-level structural metrics to the surrounding SAR signal, which reflects the local canopy context.

2.5 LiDAR Structural Variables

ALS-derived canopy metrics from the 2021 data, including plant area index (PAI) and vertical complexity index (VCI) rasters (1 m spatial resolution), were used to characterize canopy density and structural complexity. The mean PAI and VCI values were extracted within a 5 m radius around the tree location to show the vegetation density around the tree.

TLS-derived (LiPhe) canopy metrics from 2021, 2023, and 2025, were extracted for all 11 trees. Horizontal crown area (m^2) and tree height (99.5%) were derived from TLS point clouds that were used as TreeQSM inputs using the processing pipeline from LiPheKit (Wittke et al., 2024). Tree height was estimated as the difference between an upper height percentile of points and the local ground height from the DTM. Crown area was estimated using an alpha shape in the xy-plane.

3. Results

3.1 TreeQSM-Derived Branch Allocation Shifts

Tree–level branch allocation shifts show clear variability across individuals and between time periods (Fig. 1).

During 2021–2023 (Fig. 1A), the largest changes are observed in SBF, with 36.4% of the trees exhibiting marked decreases (IDs 3, 4, 7, and 9), while 45.5% of the trees show moderate increases (IDs 1, 2, 5, 8, and 10). Changes in DVF are mixed in direction, with both positive and negative shifts across trees. TCV and RBH exhibit smaller magnitude changes overall, with no consistent directional pattern. Changes in VWMD are minimal across all trees.

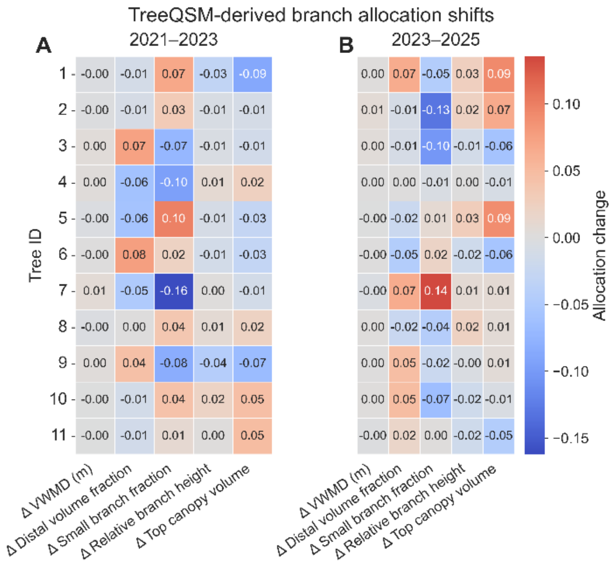

Figure 1. TreeQSM–derived branch allocation shifts per tree between (A) 2021–2023 and (B) 2023–2025.

During 2023–2025 (Fig. 1B), variability in SBF remains high, with both strong increases (e.g., ID 7) and decreases (e.g., IDs 2 and 3). Compared to the earlier period, 2 more trees show positive changes in TCV. Changes in DVF continue to vary in direction among individuals. As in the previous interval, RBH changes are generally small, and VWMD remains close to zero for most trees.

Across both periods, the magnitude of change is greatest for SBF, while VWMD and RBH exhibit comparatively limited variation. Most trees changed the direction of allocation between periods, indicating that these patterns were not fixed across time. Substantial heterogeneity among trees is evident for most allocation metrics.

3.2 Correlations

Spearman rank correlations were used to assess associations between variables. This non-parametric approach is appropriate given the small sample size and the absence of assumptions regarding the linearity or normality, allowing detection of monotonic relationships between the variables. The correlations reveal strong associations among TreeQSM–derived allocation metrics during 2021–2023 (Table 1).

The strongest relationship is observed between ΔVWMD and small branch fraction (ΔSBF) ($\rho = -0.92$, $p < 0.001$), indicating that increases in VWMD are associated with a reduced contribution of small-diameter branches to total branch volume. In addition, relative branch height (ΔRBH) and top canopy volume (ΔTCV) are positively correlated ($\rho = 0.91$, $p < 0.001$), indicating that shifts toward higher relative branch height are associated with an increasing proportion of branch volume located in the upper canopy. Moderate negative correlations are observed between distal volume fraction (ΔDVF) and both ΔRBH ($\rho = -0.45$) and ΔTCV ($\rho = -0.43$), indicating that greater allocation to distal branches corresponds to shifts toward lower average vertical position of branch volume and toward a smaller proportion of branch volume in the upper canopy.

Among SAR–derived variables, Δα shows a strong negative correlation with ΔVWMD ($\rho = -0.81$, $p < 0.01$) and a positive correlation with ΔSBF ($\rho = 0.75$, $p < 0.01$), indicating that shifts toward complex scattering are strongly associated with shifts toward smaller-diameter branches and a greater proportion of fine branching.

ΔH is also negatively correlated with ΔVWMD ($\rho = -0.55$, $p < 0.1$). Changes in C_{22}–C_{11} are also negatively associated with ΔVWMD ($\rho = -0.53$, $p < 0.1$). This indicates that increasing heterogeneity of scattering (ΔH) and increasing relative dominance of cross-polarized (volume) scattering (ΔC_{22}–C_{11}) are associated with decreases in the contribution of large-diameter branches to total branch volume, although these relationships are weak ($p < 0.1$).

	ΔVWMD	ΔDVF	ΔSBF	ΔRBH	ΔTCV
ΔVWMD					
ΔDVF	0.13				
ΔSBF	–0.92***	0.02			
ΔRBH	0.10	–0.45	–0.13		
ΔTCV	0.07	–0.43	–0.15	0.91***	
$\Delta C_{22} - C_{11}$	–0.53†	0.23	0.40	–0.26	–0.20
ΔC_{11}	0.42	0.12	–0.37	–0.15	–0.23
ΔC_{22}	–0.08	0.28	–0.02	–0.29	–0.40
ΔH	–0.55†	–0.29	0.45	–0.30	–0.33
Δα	–0.81**	–0.24	0.75**	0.11	0.15
PAI	–0.76**	0.09	0.59†	–0.28	–0.14
VCI	–0.73*	0.01	0.67*	0.00	0.16
Δh99.5	–0.11	0.45	0.22	–0.44	–0.17
ΔCA	0.64*	0.15	–0.63*	–0.52	–0.60†

Table 1. Spearman correlations for all metrics with TreeQSM–derived branch allocation shifts (2021 – 2023). *** = $p < 0.001$, ** = $p < 0.01$, * = $p < 0.05$, † = $p < 0.1$. SAR-variables: ΔC_{22} – C_{11} to Δα. ALS-variables: PAI and VCI. TLS-variables: Δh99.5 and ΔCA.

ALS–derived metrics also exhibit significant relationships with allocation shifts. PAI and VCI are both negatively correlated with ΔVWMD ($\rho = -0.76$ and -0.73, respectively; $p < 0.01$ and $p < 0.05$) and positively correlated with ΔSBF ($\rho = 0.59$ and 0.67; $p < 0.1$ and $p < 0.05$), indicating that higher values of PAI and VCI are associated with shifts toward smaller-diameter branches and a greater proportion of fine branches.

Among TLS-derived tree structural attributes, changes in crown area (ΔCA) are positively associated with ΔVWMD ($\rho = 0.64$, $p < 0.05$) and negatively associated with ΔSBF ($\rho = -0.63$, $p < 0.05$) and ΔTCV ($\rho = -0.60$, $p < 0.1$), indicating that increases in crown area are weakly associated with greater contribution of large-diameter branches, reduced fine branching, and reduced allocation of branch volume to the upper canopy.

During 2023–2025, correlations among allocation metrics are generally weaker than in the previous period, although some key relationships persist (Table 2).

The strong negative association between ΔVWMD and ΔSBF remains ($\rho = -0.92$, $p < 0.001$), consistent with 2021–2023. In contrast to the earlier period, the previously strong positive correlation between ΔRBH and ΔTCV is reduced ($\rho = 0.82$, $p < 0.01$). Other relationships are comparatively weak.

	ΔVWMD	ΔDVF	ΔSBF	ΔRBH	ΔTCV
ΔVWMD					
ΔDVF	–0.18				
ΔSBF	–0.92***	–0.07			
ΔRBH	0.15	–0.10	0.02		
ΔTCV	0.05	0.27	–0.05	0.82**	
$\Delta C_{22} - C_{11}$	0.38	0.02	–0.45	–0.27	–0.25
ΔC_{11}	–0.07	0.19	–0.07	0.08	0.23
ΔC_{22}	0.42	0.25	–0.58†	–0.25	–0.14
ΔH	0.22	0.12	–0.25	–0.48	–0.46
Δα	0.20	0.06	–0.17	–0.39	–0.48
Δh99.5	–0.28	–0.02	0.35	0.28	0.31
ΔCA	0.05	0.45	–0.24	–0.48	–0.29

Table 2. Spearman correlations for all metrics with TreeQSM–derived branch allocation shifts (2023 – 2025). *** = $p < 0.001$, ** = $p < 0.01$, * = $p < 0.05$, † = $p < 0.1$. SAR-variables: $\Delta C_{22} - C_{11}$ to Δα. TLS-variables: Δh99.5 to ΔCA.

Associations between SAR variables and allocation shifts are also reduced in 2023–2025 compared to 2021–2023. Δα and ΔH, which previously showed strong relationships with ΔVWMD and ΔSBF, exhibit weaker correlations in this period. For example, Δα shows only weak correlations with ΔVWMD ($\rho = 0.20$) and ΔSBF ($\rho = -0.17$). Similarly, ΔH shows moderate negative correlations with ΔRBH ($\rho = -0.48$) and ΔTCV ($\rho = -0.46$), but weaker associations with other allocation variables.

The other metrics also show less consistent relationships compared to the earlier period. ΔCA exhibits a moderate positive correlation with ΔDVF ($\rho = 0.45$) and a negative correlation with ΔRBH ($\rho = -0.48$).

Overall, compared to 2021–2023, the 2023–2025 period is characterized by fewer strong and significant correlations with generally lower Spearman’s ρ values, higher p-values, and less consistent relationships across variables.

3.3 Scatterplots of Significant Correlations

Scatterplots of significant correlations (Figs. 2–3) reveal consistent monotonic relationships among variables, with variation occurring along continuous gradients rather than forming discrete clusters.

Among TreeQSM-derived metrics (Fig. 2), relationships are tightly constrained. The ΔVWMD–ΔSBF relationship forms a pronounced inverse pattern across both periods, with data points closely aligned along a narrow diagonal. Similarly, ΔRBH and ΔTCV exhibit a clear positive relationship, with strong alignment of observations, although dispersion increases slightly in 2023–2025, particularly at lower values.

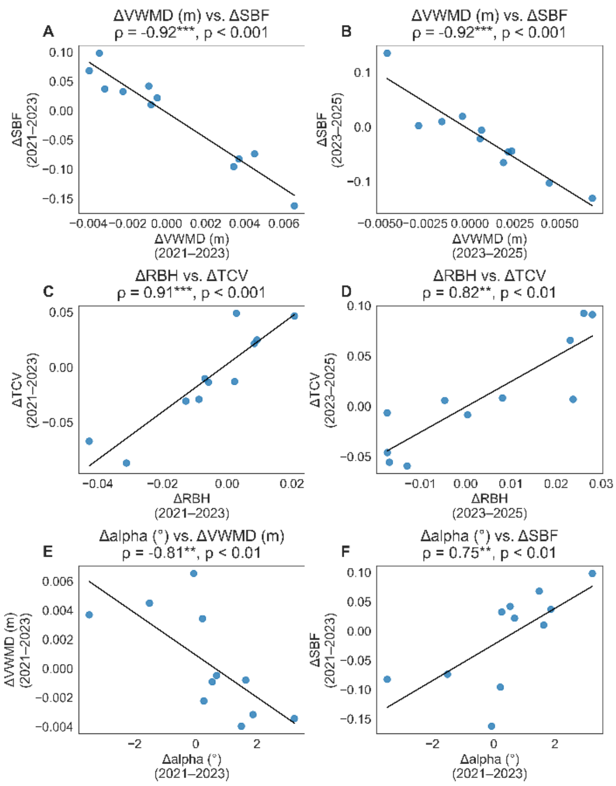

Figure 2. Significant correlations ($p < 0.001$ and < 0.01) among TreeQSM–derived branch allocation shifts and with SAR α shift.

SAR-derived Δα (Fig. 2) maintains clear monotonic relationships with allocation metrics but with greater spread compared to TreeQSM-derived relationships. The association with ΔVWMD shows increased dispersion around the fitted trend, while the relationship with ΔSBF is more tightly structured, with observations more consistently aligned along the regression line. In both cases, variability remains continuous, with no evidence of clustering.

In contrast, ALS-derived metrics and structural variables (Fig. 3) exhibit broader dispersion. While monotonic trends are still evident, observations are less tightly constrained and show greater variability around the fitted relationships. The associations involving PAI and VCI from 2021 (Fig. 3A–C) display relatively clear gradients but with wider spread than those observed for TreeQSM-derived metrics. TLS-derived structural variables, including crown area (Fig. 3D–E), show the greatest dispersion, with points more loosely distributed and increased variability at intermediate values.

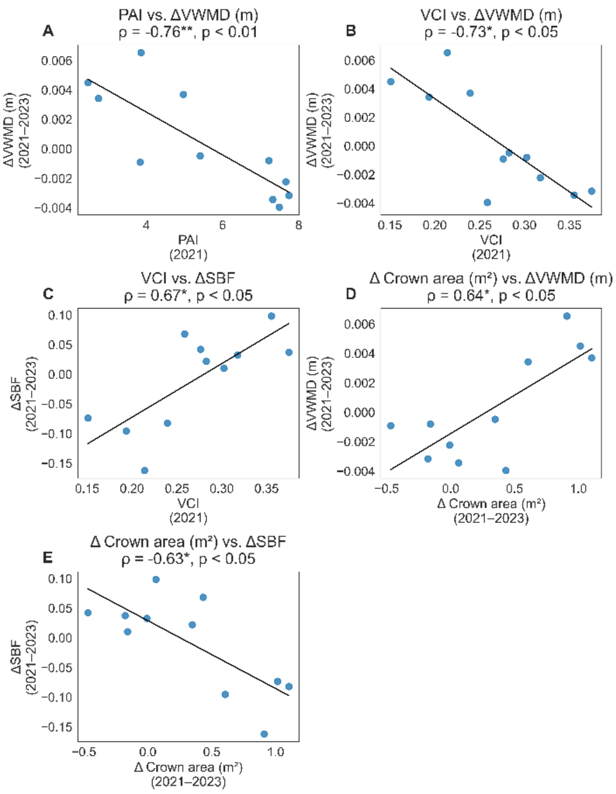

Figure 3. Significant correlations (p < 0.01 and < 0.05) between TreeQSM-derived branch allocation shifts and structural variables.

Overall, the scatterplots indicate a gradient in relationship strength, from tightly constrained patterns among TreeQSM-derived metrics to progressively greater dispersion in structural variables, while maintaining continuous monotonic behavior across all relationships.

3.4 Magnitudes and Scale of Observed Changes

TreeQSM-derived allocation shifts exhibit consistently small absolute magnitudes, with response variables tightly centered around zero. ΔVWMD shows the narrowest range (approximately ± 0.005 m), indicating millimeter-scale variation, while ΔRBH is similarly constrained (~ –0.04 to 0.02). ΔSBF spans a broader but still limited range (~ –0.15 to 0.10), similar to ΔTCV (~ –0.05 to 0.10).

In contrast, predictor variables operate across more heterogeneous scales. Structural metrics such as crown area (~0.5–1.0 m^2) show moderate dispersion, while ALS-derived indices differ in scale, with PAI ranging from approximately 2 to 8 and VCI from 0.15 to 0.35. The SAR-derived Δα spans a comparatively wide range (± 3 °), although values remain centered around zero.

4. Discussion

4.1 Coordination and Trade-offs in Silver Birch Branch Allocation

The strong and persistent negative relationship between ΔVWMD and ΔSBF indicates a consistent trade-off between structural reinforcement and exploratory growth. Increases in volume-weighted mean diameter coincide with reductions in the proportion of small branches, suggesting allocation toward thicker, load-bearing structures at the expense of finer branching. This pattern is consistent with a shift from exploratory to structural investment within the crown.

At the same time, the positive association with ΔRBH and ΔTCV suggests coordinated vertical and volumetric expansion of the canopy. Trees increasing their top canopy volume also tend to redistribute branch mass upward, indicating a linked strategy of vertical crown development rather than independent structural adjustments.

Despite these consistent pairwise relationships, the heatmap (Fig. 1) reveals substantial inter-tree variability, with no uniform direction of allocation between periods, indicating that allocation strategies are not fixed but responsive to changing conditions. These findings support the interpretation of branch allocation as a continuous and dynamic process, rather than a set of discrete structural response types.

4.2 SAR Sensitivity to Structural Allocation Dynamics

SAR-derived Δα exhibits strong and consistent associations with TreeQSM-derived allocation shifts during 2021–2023 with ΔVWMD and ΔSBF. While SAR has been used to characterize forest structure (e.g., Dostálová et al., 2018; Rüetschi et al., 2018), these results suggest a more specific and previously underexplored sensitivity: radar backscatter seems to respond to internal redistribution of branch material within the canopy, rather than only to bulk structural properties such as biomass or canopy height.

Despite the millimeter-scale magnitude of ΔVWMD, these changes reflect coordinated shifts in branch size distribution that modify canopy scattering structure. SAR responds to this collective reorganization rather than individual branch dimensions. Importantly, this response reflects the integrated canopy signal within the SAR footprint, rather than an isolated tree response, linking branch-level allocation dynamics to the surrounding local canopy context.

The observed relationships indicate that shifts between fine and coarse branching, captured by both ΔVWMD and ΔSBF, are reflected in changes in scattering mechanisms. This implies that SAR sensitivity is driven more by the spatial allocation of biomass within the canopy than by total biomass alone. Such internal allocation dynamics are typically considered sub-canopy-scale processes, requiring detailed 3D reconstruction methods such as QSM. Notably, these patterns are detected using Sentinel-1 SAR at 10 m spatial resolution, indicating that branch-level structural reorganization affects the measured SAR signal even at satellite scale.

The weakening of these relationships during 2023–2025 indicates that this sensitivity is conditional, with increased variability in SAR feature trajectories likely reflecting external influences such as moisture or phenological changes that modulate the structural signal. More studies using multivariable analyses are needed in the future.

4.3 Comparison with ALS-Derived Structural Metrics

ALS-derived metrics (PAI and VCI) also exhibit significant relationships with ΔVWMD and ΔSBF, suggesting that initial canopy density and vertical structure are associated with subsequent allocation shifts (Korpelainen et al., 2026). In contrast to SAR-derived parameters, these metrics represent the aggregated structural state of the canopy at a single time point, integrating the spatial distribution of foliage and woody components over larger scales.

As such, these ALS-derived variables from 2021 do not capture temporal changes in canopy structure but instead describe the structural context within which branch allocation shifts occur. The observed relationships therefore indicate associations between initial canopy conditions and later allocation dynamics, rather than a direct response of the ALS signal to structural reorganization.

4.4 Structural Context

Local TLS-derived structural context variables also exhibit meaningful associations with allocation shifts. Crown area change is positively related to ΔVWMD and negatively to ΔSBF, indicating that trees with expanding crowns tend to invest more in structural thickening rather than fine branching. Although crown expansion is typically linked to exploratory growth, the observed pattern suggests that expansion is accompanied by structural reinforcement rather than increased fine branching.

4.5 Implications for Multi-Scale Forest Monitoring

The results demonstrate that branch-scale, tree-level growth allocation dynamics can be linked to aerial and satellite observations, particularly SAR-derived scattering parameters. This suggests that structural reorganization within individual tree crowns may be linked to satellite observations at regional or even global scales. SAR can provide information beyond conventional structural descriptors, capturing aspects of internal canopy organization and redistribution of biomass. This extends the applicability of SAR from static characterization of forest structure toward monitoring dynamic structural processes.

In contrast, ALS-derived metrics and local TLS-derived structural variables provide complementary context, reflecting canopy density, vertical structure, and competitive environment. Together, these results highlight the value of integrating multi-modal and multi-scale data sources.

5. Conclusions

This study demonstrates that tree-level branch allocation shifts, derived from multi-temporal TreeQSM models, are systematically related to both SAR and ALS observations. Although the observed allocation shifts are small in absolute magnitude, they represent fine-scale structural adjustments that are consistently reflected across datasets. A clear trade-off between structural reinforcement and exploratory branching is observed, reflected in strong relationships between volume-weighted mean diameter and small branch fraction.

SAR-derived α shows particularly strong associations with these allocation shifts, indicating sensitivity to internal redistribution of branch material within the canopy. Notably, these relationships are detectable using Sentinel-1 data at 10 m spatial resolution, linking branch-level structural dynamics to satellite-scale observations within the surrounding canopy context.

While ALS-derived metrics and structural context variables provide additional insight into canopy density and competition, SAR appears more directly responsive to internal structural reorganization. However, this sensitivity is conditional. The limited sample size constrains the generality of the observed relationships, and the spatial resolution of SAR implies that the extracted signals represent integrated responses from the surrounding canopy and ground rather than isolated tree-level measurements. In addition, external factors such as moisture conditions and phenological variability can modulate or obscure the structural signal, as reflected in the weakening correlations during the 2023–2025 period.

Overall, the results highlight the potential of integrating detailed 3D tree models with multimodal and multiscale remote sensing observations to monitor subtle, dynamic changes in forest structure across scales. Further work with larger datasets, extended time series, and improved separation of structural and environmental effects is needed to confirm the robustness of these relationships.

References

Bruggisser, M., Hollaus, M., Kükenbrink, D., Pfeifer, N., 2019. COMPARISON OF FOREST STRUCTURE METRICS DERIVED FROM UAV LIDAR AND ALS DATA. *ISPRS Ann. Photogramm. Remote Sens. Spatial Inf. Sci.* IV-2/W5, 325–332. doi.org/10.5194/isprs-annals-IV-2-W5-325-2019.

Campos, M., Litkey, P., Wang, Y., Chen, Y., Hyyti, H., Hyyppä, J., Puttonen, E., 2021. A Long-Term Terrestrial Laser Scanning

Measurement Station to Continuously Monitor Structural and Phenological Dynamics of Boreal Forest Canopy. *Front. Plant Sci.* 11. doi.org/10.3389/fpls.2020.606752.

CloudCompare, 2021. CloudCompare Software, Version 2.12.4. CloudCompare. http://www.cloudcompare.org/ (18 March 2026).

Cloude, S.R., Pottier, E., 1997. An entropy based classification scheme for land applications of polarimetric SAR. *IEEE Trans. Geosci. Remote Sens.* 35(1), 68–78. doi.org/10.1109/36.551935.

Dostálová, A., Wagner, W., Milenković, M., Hollaus, M., 2018. Annual seasonality in sentinel-1 signal for forest mapping and forest type classification. *Int. J. Remote Sens.* 39, 7738–7760. doi.org/10.1080/01431161.2018.1479788.

Junttila, S., Campos, M., Hölttä, T., Lindfors, L., El Issaoui, A., Vastaranta, M., Hyyppä, H., Puttonen, E., 2022. Tree Water Status Affects Tree Branch Position. *Forests* 13(5), 728. doi.org/10.3390/f13050728.

Korpelainen, T., Batista Campos, M., Yrttimaa, T., Junttila, S., Kukko, A., Hyyppä, J., Wang, Y., Puttonen, E., 2026. Uncovering growth dynamics in Scots pine through the detection of the onset of height growth using near-daily terrestrial laser scanning time series. *Ecol. Informatics.* 95, 103685. doi.org/10.1016/j.ecoinf.2026.103685.

Mäkinen, K., 2024. SARP. https://gitlab.com/fgi_nls/public/sarp (18 March 2026).

Proisy, C., Mougin, E., Dufrêne, E., Le Dantec, V., 2000. Monitoring seasonal changes of a mixed temperate forest using ers sar observations. *IEEE Trans. Geosci. Remote Sens.* 38, 540–552. doi.org/10.1109/36.823949.

Raumonen, P., Åkerblom, M., 2024. InverseTampere/TreeQSM: Version 2.4.1, Zenodo. doi.org/10.5281/zenodo.6539580.

Rüetschi, M., Schaepman, M.E., Small, D., 2018. Using multitemporal sentinel-1 c-band backscatter to monitor phenology and classify deciduous and coniferous forests in Northern Switzerland. *Remote Sens.* 10, 55. doi.org/10.3390/rs10010055.

Seidel, D., Leuschner, C., Müller, A., Krause, B., 2011. Crown plasticity in mixed forests – Quantifying tree individual response to environmental variability. *For. Ecol. Manag.* 262(3), 420–428. doi.org/10.1016/j.foreco.2011.03.008.

Sorokina, H.E., Campos, M., Raumonen, P., Shcherbacheva, A., Echriti, R., Hyyppä, J., Puttonen, E., Wang, Y., 2026. Boundary conditions for studying branch-scale tree growth strategies using tree quantitative structure model time series. *Remote Sens. Environ.* 333, 115105. doi.org/10.1016/j.rse.2025.115105.

The MathWorks, Inc., 2024. MATLAB version: 24.2 (R2024b). https://www.mathworks.com (accessed 20 May 2026)

Wilkes, P., Shenkin, A., Disney, M., Malhi, Y., Bentley, L.P., Vicari, M.B., 2021. Terrestrial laser scanning to reconstruct branch architecture from harvested branches. *Methods Ecol. Evol.* 12(12). 2487–2500. doi.org/10.1111/2041-210X.13709.

Wittke, S., Campos, M., Ruoppa, L., Echriti, R., Wang, Y., Gołoś, A., Kukko, A., Hyyppä, J., Puttonen, E., 2024. LiPheStream - a 18-month high spatiotemporal resolution point cloud time series of boreal trees from Finland. *Sci. Data*, 11, 1281. doi.org/10.1038/s41597-024-04143-w.